DOI: 10.17344/acsi.2019.5630 *Acta Chim. Slov.* **2020,** *67,* 622–628

Scientific paper

Magnetic, Photoluminescent and Semiconductor Properties of a 4*f*-5*d* Bromide Compound

Wen-Tong Chen*

[1] *Institute of Applied Chemistry, School of Chemistry and Chemical Engineering, Jinggangshan University, Ji'an, Jiangxi 343009, China*

[2] *Department of Ecological and Resources Engineering, Fujian Key laboratory of Eco-Industrial Green Technology, Wuyi University, Wuyishan, Fujian 354300, China*

[3] *State Key Laboratory of Structural Chemistry, Fujian Institute of Research on the Structure of Matter, Chinese Academy of Sciences, Fuzhou, Fujian 350002, China*

** Corresponding author: E-mail: wtchen_2000@aliyun.com*
Tel.: +86(796)8100490; fax +86(796)8100490

Received: 10-14-2019

Dedicated to Professor Jin-Shun Huang on the occasion of his 80th birthday.

Abstract

A novel 4*f*–5*d* material $(HgDy_6Br_{12})Hg_8Br_{24}$ (**1**) is prepared by hydrothermal reactions and structurally characterized by single crystal X-ray diffraction. Compound **1** is characterized by a two-dimensional (2*D*) layered structure. A photoluminescence measurement with solid-state samples shows that this compound exhibits a strong emission in the blue region. A narrow optical band gap of 1.97 eV is revealed by a solid-state UV/Vis diffuse reflectance spectrum. The variable-temperature magnetic susceptibility obeys the Curie-Weiss law ($\chi_m = c/(T-\theta)$) with $C = 0.78$ K and a Weiss constant $\theta = -0.38$ K as revealed by the magnetic measurements, suggesting the existence of an antiferromagnetic interaction.

Keywords: Lanthanide; mercury; magnetism; photoluminescence; semiconductor

1. Introduction

Lanthanide compounds have recently gained more and more attention because of their attractive photoluminescent, magnetic, catalytic and other performances.[1–9] Nowadays, scientists from chemistry and material domains have completed a large number of explorations on different lanthanide compounds, in order to find out their application potentials in luminescent probes, light-emitting diodes (LEDs), electrochemical displays, and magnetic materials and so on.[10–14] The attractive photoluminescent and magnetic performances of lanthanide compounds mainly come from the abundant 4f electrons of lanthanide (LN) ions. Generally speaking, lanthanide compounds may show strong photoluminescence only when the electronic transitions of the 4f electron of the lanthanide ion can efficiently happen. Moreover, a number of lanthanide compounds are interesting due to their fascinating magnetic and magneto-optical performances.[15–20] As a result, a great number of researchers have devoted themselves into the exploration of design, preparation and characterization of new lanthanide-containing magnetic compounds. However, the semiconductor performances of lanthanide compounds are rarely explored yet in comparison with the studies on the photoluminescent and magnetic properties of the lanthanide materials.[21]

Group 12 (IIB) metals are zinc, cadmium and mercury and they have drawn much attention due to the following aspects: various coordination modes, photoluminescent and photoelectric properties, as well as the vital role played in the biosystem by zinc.[22,23] The IIB metals are also very important components in semiconductor compounds and, up to date, many semiconductor compounds containing IIB metals have so far been reported.[24–27] Since many years ago, photoluminescent, magnetic and semiconductor compounds have become one of research hotspots. The LN-IIB-VIIA (LN = lanthanide, VIIA = halogen) compounds have become one of research hotspots

due to the attractive crystal structure, photoluminescence, magnetism and semiconductor performances. In this work, the synthesis, crystal structure, gas adsorption, magnetism, photoluminescence, and semiconductor performances of a 4*f*–5*d* material ($HgDy_6Br_{12}$)Hg_8Br_{24} (**1**) with a 2-D layered structure are reported. It should be pointed out that some ternary LN-IIB-VIIA compounds have thus far been reported,[28–32] but most of them are fluorides and an iodide with cadmium or zinc.

2. Experimental Section

2. 1. Materials and Characterization

The chemicals were purchased via commercial sources and directly used. The photoluminescence experiments were carried out on a F97XP photoluminescent spectrometer. A solid-state UV/vis diffuse reflectance spectrum was measured at room temperature on a computer-controlled TU1901 UV/vis spectrometer equipped with an integrating sphere in the wavelength range of 190–900 nm. The barium sulfate powder was applied as a reference of 100% reflectance, on which the finely ground powder sample was daubed. Variable-temperature magnetic susceptibility and field dependence magnetization measurements of the title compound on polycrystalline samples were carried out on a PPMS 9T Quantum Design SQUID magnetometer and the diamagnetism correction of the magnetic data was calculated from the Pascal's constants.

2. 2. Synthesis of 1

A mixture of $Dy(NO_3)_3 \cdot 6H_2O$ (1 mmol, 458 mg), $HgBr_2$ (1 mmol, 360 mg) and distilled water (10 mL) was sealed into a 23 mL Teflon-lined stainless steel vessel. The vessel was heated to 473 K and kept there for one week under autogenous pressure. When the vessel was slowly cooled to room temperature, colorless block-like crystals were obtained. The yield was 21% based on $HgBr_2$.

2. 3. Crystal Structure Determination and Refinement

A carefully selected single crystal (0.08 × 0.07 × 0.06 mm^3) was adhered onto the tip of a glass fiber and then mounted to a SuperNova CCD diffractometer. The X-ray source is graphite monochromated Mo-*Kα* radiation with the λ = 0.71073 Å. The intensity data were obtained at 293(2) K with the ω scan mode. For data reduction and empirical absorption correction, CrystalClear software was applied. The crystal structure of the title compound was solved by using the direct methods. The final structure was refined on F^2 by full-matrix least-squares using the Siemens SHELXTL^{TM} V5 crystallographic software package. All of the atoms were generated on the difference Fourier maps and refined anisotropically. The high max./min. residual electron density is ghost peak around the heavy atom. The crystal data as well as the details of the data collection and refinement are given in Table 1, while the selected bond lengths and bond angles are listed in Table 2.

Table 1. Crystal data and structure refinement details.

Formula	$Br_{36}Dy_6Hg_9$
Mr	5656.71
Crystal system	orthorhombic
Space group	*Pbam*
a (Å)	13.0997(11)
b (Å)	13.6459(13)
c (Å)	27.906(3)
V (Å^3)	4988.4(8)
Z	2
$2\theta_{max}$ (°)	50
Reflections collected	12182
Independent, observed reflections (R_{int})	3855, 2167 (0.0437)
$d_{calcd.}$ (g/cm^3)	3.741
μ (mm^{-1})	31.850
F(000)	4722
R_1, wR_2	0.1122, 0.3031
S	1.032
$\Delta\rho$ (max, min) (e/Å^3)	1.956, –2.820

Table 2. Selected bond lengths (Å) and bond angles (°).

Hg1-Br5	2.400(4)	Dy2-Br4	3.349(3)
Hg1-Br6	2.748(4)	Dy2-Br4#4	3.349(3)
Hg1-Br7	2.617(5)	Dy3-Br4	2.417(3)
Hg1-Br8	2.767(6)	Dy3-Br4#7	2.417(3)
Hg2-Dy2#1	2.961(2)	Dy3-Br5	3.278(4)
Hg2-Dy2	2.961(2)	Dy3-Br5#7	3.278(4)
Hg2-Dy1#2	3.037(2)	Dy1-Dy2	3.468(3)
Hg2-Dy1#3	3.037(2)		
Hg2-Dy3	3.431(2)	Br5-Hg1-Br7	124.2(2)
Hg2-Dy3#1	3.431(2)	Br5-Hg1-Br8	114.7(2)
Hg3-Br10	2.370(4)	Br7-Hg1-Br8	102.60(18)
Hg3-Br11	2.397(4)	Br5-Hg1-Br6	121.91(18)
Dy1-Br1#4	2.390(3)	Br7-Hg1-Br6	94.15(14)
Dy1-Br1	2.390(3)	Br8-Hg1-Br6	93.27(16)
Dy1-Br2#5	3.425(6)	Br10-Hg3-Br11	174.89(19)
Dy1-Br3#6	3.310(6)	Br2-Dy2-Br3	163.63(19)
Dy2-Br2	2.420(5)	Br4-Dy3-Br4#7	173.99(19)
Dy2-Br3	2.398(5)	Br4-Dy3-Br5	90.74(13)

Symmetry transformations used to generate equivalent atoms: #1 $-x+3, -y-2, -z-1$; #2 $-x+7/2, y+½, z$; #3 $x-½, -y-5/2, -z-1$; #4 $x, y, -z-1$; #5 $x+½, -y-5/2, -z-1$; #6 $-x+7/2, y-½, z$; #7 $-x+3, -y-2, z$.

3. Results and Discussion

As revealed by the single crystal X-ray diffraction, the title compound crystallizes in the space group *Pbam* of the orthorhombic system with two formula units in one cell. The asymmetric unit of compound **1** includes

three mercury ions (Hg1 in full occupancy, Hg2 in 0.25 occupancies, Hg3 in full occupancy), three dysprosium ions (Dy1, Dy2, Dy3; all in 0.5 occupancies) and eleven bromine ions (from Br1 to Br11; Br2, Br3, Br6, Br9 in 0.5 occupancies, while others in full occupancy), as depicted in Fig. 1. Most of the crystallographically independent ions are located in the general positions, but all dysprosium ions as well as Hg2, Br2, Br3, Br6, and Br9 ions are resided at the special positions. Results of the bond valence calculations indicate that all dysprosium ions are in +3 oxidation state (Dy1: 3.395, Dy2: 3.246, Dy3: 3.231), while mercury ions Hg1 and Hg3 are in +2 oxidation state (Hg1: 2.318, Hg3: 2.093).[33,34] The bond valence of Hg2 is not available because it contains only metal-metal bonds.

The Hg1 ion is coordinated by four bromine atoms and yields a slightly distorted $HgBr_4$ tetrahedron with the bond angles of Br-Hg1-Br locating in the span of 93.27(16)° to 124.2(2)° and the bond lengths of Hg-Br locating in the range of 2.400(4) Å to 2.767(6) Å, which is comparable with those reported previously.[35–37] Differently, the Hg2 ion is surrounded by six dysprosium ions and forms a $HgDy_6$ octahedron. The distances of Hg-Dy are in the range of 2.961(2) Å to 3.431(2) Å. The Hg3 ion, however, is coordinated by two bromine ions to give an almost linear geometry of $HgBr_2$ with the bond angle of Br10-Hg3-Br11 being of 174.89(19)° and the bond lengths of Hg-Br being of 2.370(4) Å and 2.397(4) Å. All dysprosium ions are surrounded by four bromine ions. The bond distance of Dy-Br is located in the range of 2.390(3) Å to 3.425(6) Å. The bond angle of Br-Dy-Br is in the span of 90.74(13)° to 173.99(19)°. Two $HgBr_4$ tetrahedra connect together via a corner-sharing bromide ion to yield a dimer, as shown in Fig. 2a. The dimers then interconnect together via the bromide ions to form a one-dimensional (1-D) chain running along the *a* axis. The chains and $HgBr_2$ moieties are in the same plane and form an Hg-Br layer (Fig. 2a and the purple layers in Fig. 3). The $HgDy_6$ octahedra interconnect together via Dy-Dy interactions to yield a two-dimensional (2-D) Hg-Dy-Br layer extending parallel to the *ab* plane. The Dy-Dy distance is 3.468(3) Å, which is comparable with those reported in the literature.[38,39] These Hg-Br layers and Hg-Dy-Br layers stack along the *c* axis in the number of 2-1-2 to yield a crystal packing structure of compound **1**, as presented in Fig. 3.

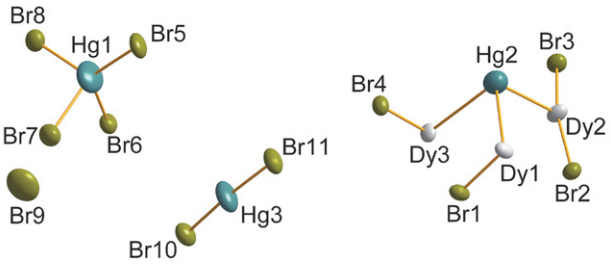

Figure 1. An ORTEP drawing of the asymmetric unit of **1** with 30% thermal ellipsoids.

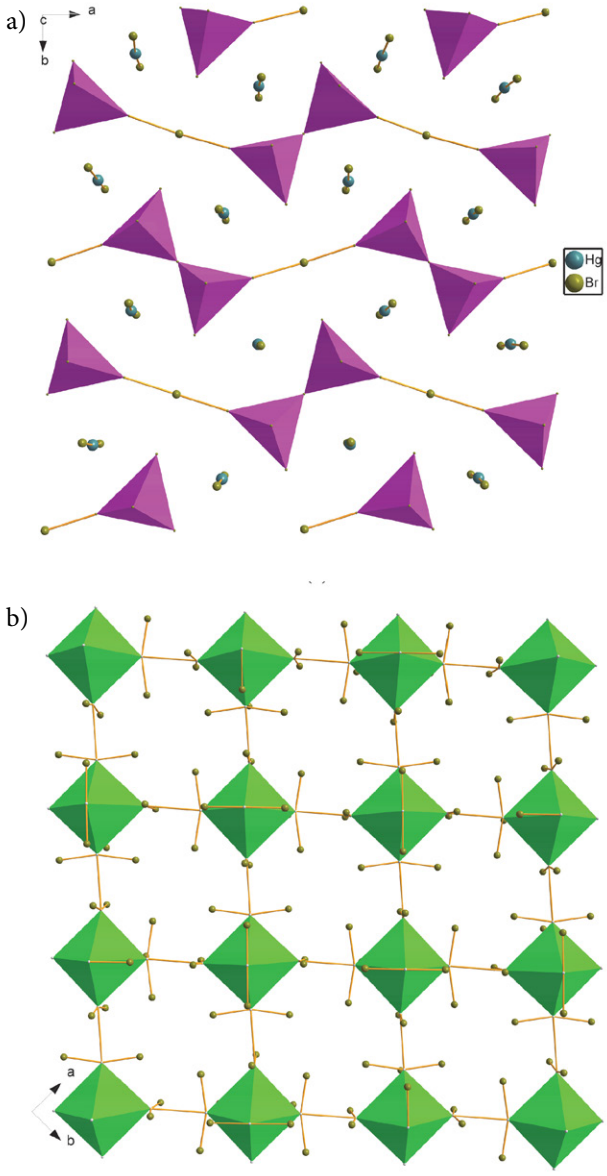

Figure 2. (a) The Hg-Br layer with the purple polyhedra representing the $HgBr_4$ tetrahedra and (b) the Hg-Dy-Br layer with the green polyhedra representing the $HgDy_6$ octahedra.

Lanthanide materials can usually exhibit photoluminescence and, nowadays, a large number of lanthanide materials have been reported for the photoluminescent performance and for potential applications as photoluminescent emitting materials like electrochemical displays, LEDs, chemical sensors and so on.[40–42] As a dysprosium-containing compound, the title compound is possible to display photoluminescence. The photoluminescence property of compound **1** was explored in the solid state at room temperature. The results of the photoluminescence experiments are given in Fig. 4. The photoluminescence spectrum of compound **1** obviously shows an effective energy absorption residing in the wavelength span of 400 to 430 nm. The photoluminescence excitation spectrum using the emission wavelength of 445 nm yields one sharp

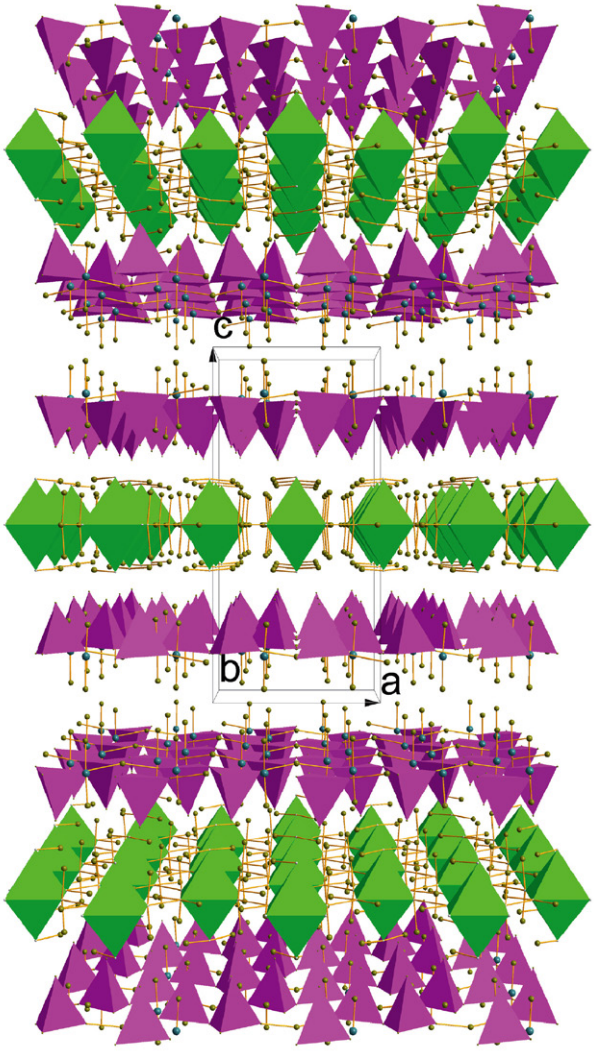

Figure 3. A packing diagram of compound **1**.

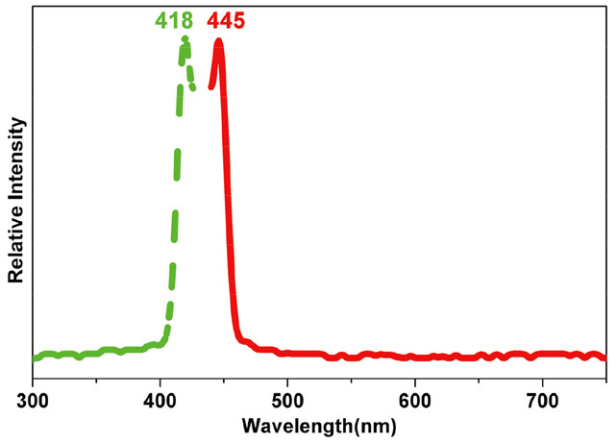

Figure 4. The solid state photoluminescence spectra of compound **1**. Green dashed line: excitation; red solid line: emission.

excitation peak at 418 nm. The corresponding photoluminescence emission spectrum of compound **1** is also measured, with the irradiation wavelength at 418 nm. The photoluminescence emission spectrum is characteristic of one sharp peak residing at 445 nm of blue region. Therefore, the title compound can be a candidate for potential blue photoluminescence materials.

Mercury is well-known as an important component of semiconductor materials. The title compound contains mercury and it is supposed to display semiconductor property. So, the solid-state UV/Vis diffuse reflectance spectrum is explored with solid state samples at room temperature and the data of the diffuse reflectance spectrum were treated using the Kubelka-Munk function, namely, $\alpha/S = (1\text{-}R)^2/2R$. In this function, α means the absorption coefficient, S is the scattering coefficient that is practically wavelength independent when the particle size is larger than 5 μm, while R is the reflectance. The optical band gap value can be determined by extrapolating from the linear part of the absorption edges of the α/S vs. energy diagram, as presented in Fig. 5. The solid-state diffuse reflectance spectrum shows that compound **1** has a narrow optical band gap of 1.97 eV and, therefore, compound **1** can be a candidate for narrow band gap semiconductor materials. The solid-state diffuse reflectance spectrum displays a slow slope of the optical absorption edge that indicates an indirect transition process.[43] The optical band gap value of 1.97 eV of compound **1** is larger than that of $CuInS_2$ (1.55 eV), CdTe (1.5 eV) and GaAs (1.4 eV) which are efficient photovoltaic materials.[44,45]

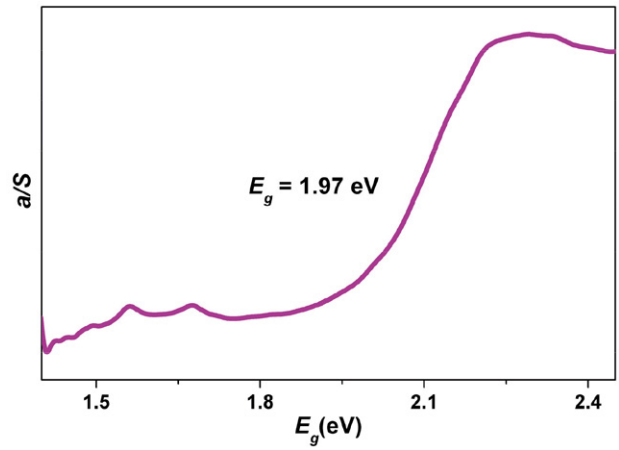

Figure 5. A solid-state diffuse reflectance spectrum for compound **1**.

Trivalent lanthanide ions-containing compounds can generally display magnetic performance.[46–48] Therefore, the title compound is supposed to exhibit magnetic behaviors. The χ_M vs. T and μ_{eff} vs. T curves for the title compound are presented in Fig. 6. The χ_M is the magnetic susceptibility per Dy-containing molecule. When the temperature is decreased, the χ_M vs. T diagram continuously increases from 0.06 emu mol^{-1} at 300 K to 0.39 emu mol^{-1} at 2 K. Such a χ_M vs. T diagram of compound **1** indicates an antiferromagnetic-like performance. The essence of this antiferromagnetic-like performance is not clear yet, but it

is supposed to be originated from the gradual thermal depopulation of the Stark components of the dysprosium ions. The magnetic susceptibility diagram agrees well with the Curie-Weiss law, namely, $\chi_m = c/(T-\theta)$. The data of the magnetic susceptibility is fitted from 300 K to 2 K using this Curie-Weiss law and it results in the value of C being of 0.78 K and a Weiss constant θ being of –0.38 K, as presented in Fig. 6. The negative Weiss constant confirms the presence of the antiferromagnetic-like performance in compound **1**. When the temperature was decreased, the μ_{eff} vs. T diagram continuously decreases from 11.89 μ_B at 300 K to 2.45 μ_B at 2 K, which also confirms the presence of the antiferromagnetic-like performance in compound **1**, as shown in Fig. 6. The field dependence of the magnetization of compound **1** was carried out at 2 K, as given in Fig. 7. This diagram shows a very small coercive field of about 40 Oe and a remnant magnetization of around 0.002 $N\beta$. The magnetization diagram increases fast with the increased field from –80 kOe to 80 kOe. A saturation value cannot be obtained even at 80 kOe. The value is 0.49 Nβ at 80 kOe.

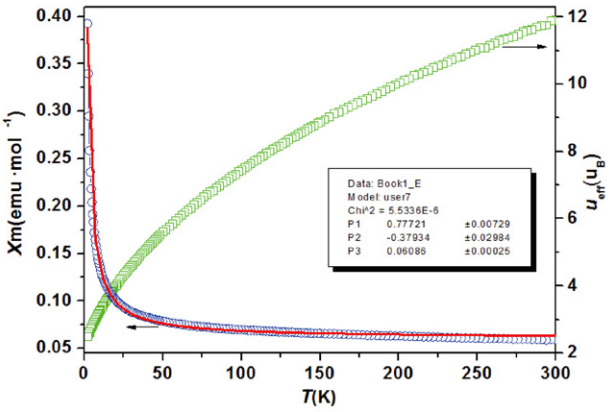

Figure 6. Thermal dependence of χ_M and μ_{eff} for **1** with the red line representing the best fitting curve

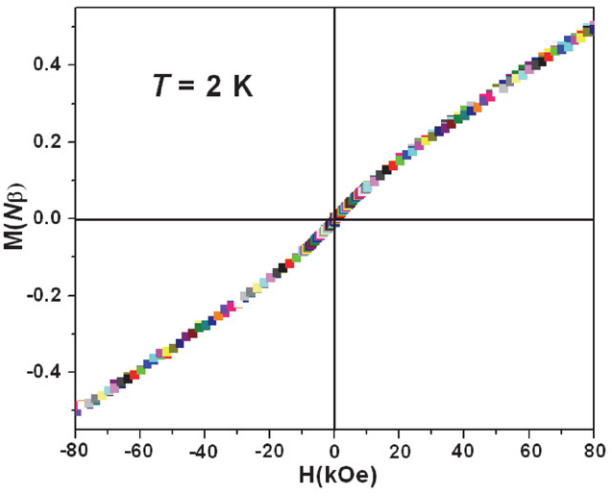

Figure 7. A curve of magnetization vs H.

4. Conclusions

A novel 4*f*-5*d* bromide compound $(HgDy_6Br_{12})Hg_8B_{r24}$ has been synthesized and structurally characterized by single crystal X-ray diffraction. This compound is characteristic of a 2-D layered structure. The solid-state photoluminescence measurement shows that it displays a strong emission in the blue region. A solid-state UV/Vis diffuse reflectance spectrum shows that this compound has a narrow optical band gap of 1.97 eV. This compound exhibits an antiferromagnetic interaction with C = 0.78 K and a Weiss constant θ = –0.38 K. As a result, this compound is probably a candidate of photoluminescence, semiconductive or magnetic materials.

Acknowledgments

Author thanks the financial support of the NSF of China (21361013), Jiangxi Provincial Department of Education's Item of Science and Technology (GJJ170637), and the open foundation (20180008) of the State Key Laboratory of Structural Chemistry, Fujian Institute of Research on the Structure of Matter, Chinese Academy of Sciences.

Supplementary Material

Crystallographic data in CIF format have been deposited with FIZ Karlsruhe with the following CSD numbers: 1947021. These data can be obtained from the Fachinformationszentrum Karlsruhe, 76344 Eggenstein-Leopoldshafen, Germany, (fax: (49) 7247-808-666; e-mail: crysdata@fiz.karlsruhe.de).

5. References

1. T. Zheng, C. Cao, P. Dong, S. Liu, F. Wang, X. Tong, J. Liao, J. Chen, H. Wen, *Polyhedron* **2016**, *113*, 96–101. **DOI:**10.1016/j.poly.2016.04.011
2. R. F. Mendes, D. Ananias, L. D. Carlos, J. Rocha, F. A. A. Paz, *Cryst. Growth Des.* **2017**, *17*, 5191–5199. **DOI:**10.1021/acs.cgd.7b00667
3. S.-J. Liu, T.-F. Zheng, J. Bao, P.-P. Dong, J.-S. Liao, J.-L. Chen, H.-R. Wen, J. Xu, X.-H. Bu, *New J. Chem.* **2015**, *39*, 6970–6975. **DOI:**10.1039/C5NJ01229E
4. P. Zhang, L. Zhang, C. Wang, S. Xue, S.-Y. Lin, J. Tang, *J. Am. Chem. Soc.* **2014**, *136*, 4484–4487. **DOI:**10.1021/ja500793x
5. S.-L. Yao, C. Cao, X.-M. Tian, T.-F. Zheng, S.-J. Liu, X.-L. Tong, J.-S. Liao, J.-L. Chen, H.-R. Wen, *ChemistrySelect* **2017**, *2*, 10673–10677. **DOI:**10.1002/slct.201702223
6. S. Han, R. Deng, X. Xie, X. Liu, *Angew. Chem. Int. Edit.* **2014**, *53*, 11702–11715. **DOI:**10.1002/anie.201403408
7. S. Liu, Y. Cui, W. Song, Q. Wang, X. Bu, *Chinese J. Inorg. Chem.* **2015**, *31*, 1894–1902.

8. B. Zhou, L. Tao, Y. Chai, S. P. Lau, Q. Zhang, Y. H. Tsang, *Angew. Chem. Int. Edit*. **2016**, *55*, 12356–12360. **DOI:**10.1002/anie.201604682
9. S.-J. Liu, S.-L. Yao, C. Cao, T.-F. Zheng, C. Liu, Z.-X. Wang, Q. Zhao, J.-S. Liao, J.-L. Chen, H.-R. Wen, *Polyhedron* **2017**, *121*, 180–184. **DOI:**10.1016/j.poly.2016.09.040
10. F. Pointillart, O. Cador, B. Le Guennic, L. Ouahab, *Coord. Chem. Rev*. **2017**, *346*, 150–175. **DOI:**10.1016/j.ccr.2016.12.017
11. H. Kuang, Z. Zhang, L. Lin, H. Chen, W. Chen, *Chinese J. Struct. Chem*. **2019**, *38*, 337–344. **DOI:**10.1016/j.ccr.2017.01.012
12. J. A. Kitchen, *Coord. Chem. Rev*. **2017**, *340*, 232–246.
13. S.-D. Han, S.-J. Liu, Q.-L. Wang, X.-H. Miao, T.-L. Hu, X.-H. Bu, *Cryst. Growth Des*. **2015**, *15*, 2253–2259. **DOI:**10.1021/acs.cgd.5b00024
14. I. A. Shkrob, M. D. Kaminski, C. J. Mertz, P. G. Rickert, M. S. Derzon, K. Rahimian, *J. Am. Chem. Soc*. **2009**, *131*, 15705–15710. **DOI:**10.1021/ja9035253
15. T.-F. Zheng, X.-M. Tian, S.-L. Yao, C. Cao, J.-B. Cai, S.-J. Liu, *J. Mol. Struct*. **2018**, *1165*, 326–331. **DOI:**10.1016/j.molstruc.2018.03.112
16. O. Ofer, J. Sugiyama, J. H. Brewer, E. J. Ansaldo, M. Mansson, K. H. Chow, K. Kamazawa, Y. Doi, Y. Hinatsu, *Phys. Rev. B* **2011**, *84*, 054428/1–054428/5. **DOI:**10.1103/PhysRevB.84.054430
17. S. Liu, X. Xie, T. Zheng, J. Bao, J. Liao, J. Chen, H. Wen, *CrystEngComm* **2015**, *17*, 7270–7275. **DOI:**10.1039/C5CE00997A
18. G. Abbas, Y. Lan, G. Kostakis, C. E. Anson, A. K. Powell, *Inorg. Chim. Acta* **2008**, *361*, 3494–3499. **DOI:**10.1016/j.ica.2008.03.024
19. A. Kirste, N. P. Kolmakova, S. Hansel, H.-U. Mueller, M. Von Ortenberg, *Physica B* **2004**, *346-347*, 191–195. **DOI:**10.1016/j.physb.2004.01.048
20. S.-J. Liu, C. Cao, S.-L. Yao, T.-F. Zheng, Z.-X. Wang, C. Liu, J.-S. Liao, J.-L. Chen, Y.-W. Li, H.-R. Wen, *Dalton Trans*. **2017**, *46*, 64–70. **DOI:**10.1039/C6DT03589B
21. N. Ahmed, J. Nisar, R. Kouser, A. G Nabi, S. Mukhtar, Y. Saeed, M. H. Nasim, *Mater. Res. Express* **2017**, *4*, 065903/1–065903/8. **DOI:**10.1088/2053-1591/aa75fc
22. J. B. Waters, R. S. P. Turbervill, J. M. Goicoechea, *Organometallics* **2013**, *32*, 5190–5200. **DOI:**10.1021/om400728u
23. B. Mohapatra, S. Verma, *Cryst. Growth Des*. **2013**, *13*, 2716–2721. **DOI:**10.1021/cg4006168
24. Y. Yoshida, H. Ito, Y. Nakamura, M. Ishikawa, A. Otsuka, H. Hayama, M. Maesato, H. Yamochi, H. Kishida, G. Saito, *Cryst. Growth Des*. **2016**, *16*, 6613–6630. **DOI:**10.1021/acs.cgd.6b01294
25. L. Zhang, H. Lin, Y. Wu, S. Zhuo, *Chem. Phys. Lett*. **2016**, *661*, 224–227. **DOI:**10.1016/j.cplett.2016.08.079
26. Y. Zeng, D. F. Kelley, *J. Phys. Chem. C* **2016**, *120*, 17853–17862. **DOI:**10.1021/acs.jpcc.6b06282
27. T. Uematsu, E. Shimomura, T. Torimoto, S. Kuwabata, *J. Phys. Chem. C* **2016**, *120*, 16012–16023. **DOI:**10.1021/acs.jpcc.5b12698
28. A. F. Konstantinova, E. A. Krivandina, D. N. Karimov, B. P. Sobolev, *Crystallogr. Rep*. **2010**, *55*, 990–994. **DOI:**10.1134/S1063774510060143
29. N. I. Sorokin, E. A. Krivandina, Z. I. Zhmurova, *Crystallogr. Rep*. **2013**, *58*, 948–952. **DOI:**10.1134/S1063774513060217
30. S. V. Kuznetsov, P. P. Fedorov, *Inorg. Mater*. **2008**, *44*, 1434–1458. **DOI:**10.1134/S0020168508130037
31. A. F. Konstantinova, T. M. Glushkova, I. I. Buchinskaya, E. A. Krivandina, B. P. Sobolev, *Crystallogr. Rep*. **2009**, *54*, 609–612. **DOI:**10.1134/S1063774509040117
32. M. Lukachuk, L. Kienle, C. Zheng, H. Mattausch, A. Simon, *Inorg. Chem*. **2008**, *47*, 4656–4660. **DOI:**10.1021/ic800024n
33. M. Kasunič, S. D. Škapin, D. Suvorov, A. Golobič, *Acta Chim. Slov*. **2012**, *59*, 117–123.
34. I. D. Brown, D. Altermat, *Acta Crystallogr. B* **1985**, *41*, 244. **DOI:**10.1107/S0108768185002063
35. S. J. Sabounchei, M. Ahmadianpoor, A. Hashemi, F. Mohsenzadeh, R. W. Gable, *Inorg. Chim. Acta* **2017**, *458*, 77–83. **DOI:**10.1016/j.ica.2016.12.023
36. J. Vallejos, I. Brito, A. Cardenas, J. Llanos, M. Bolte, M. *J. Solid State Chem.* **2015**, *223*, 17–22. **DOI:**10.1016/j.jssc.2014.03.022
37. G. Mahmoudi, A. A. Khandar, J. K. Zareba, M. J. Bialek, M. S. Gargari, M. Abedi, G. Barandika, D. Van Derveer, J. Mague, A. Masoumi, *Inorg. Chim. Acta* **2015**, *429*, 1–14. **DOI:**10.1016/j.ica.2014.12.027
38. T. Stewart, M. Nishiura, Y. Konno, Z. Hou, G. J. McIntyre, R. Bau, *Inorg. Chim. Acta* **2010**, *363*, 562–566. **DOI:**10.1016/j.ica.2009.03.024
39. K. Daub, G. Meyer, *Z. Anorg. Allg. Chem.* **2010**, *636*, 1716–1719.
40. J. J. Joos, D. Poelman, P. F. Smet, *Phys. Chem. Chem. Phys.* **2015**, *17*, 19058–19078. **DOI:**10.1039/C5CP02156A
41. Y. Zhang, W. Wei, G. K. Das, T. Yang, T. Timothy, *J. Photoch. Photobio. C.* **2014**, *20*, 71–96. **DOI:**10.1016/j.jphotochemrev.2014.06.001
42. W. G. J. H. M. van Sark, J. de Wild, J. K. Rath, A. Meijerink, R. El Schropp, *Nanoscale Res. Lett.* **2013**, *8*, 81/1–81/10.
43. F. Q. Huang, K. Mitchell, J. A. Ibers, *Inorg. Chem.* **2001**, *40*, 5123–5126. **DOI:**10.1021/ic0104353
44. P. Dürichen, W. Bensch, *Eur. J. Solid State Inorg. Chem.* **1997**, *34*, 1187–1198.
45. R. Tillinski, C. Rumpf, C. Näther, P. Duerichen, I. Jess, S. A. Schunk, W. Bensch, *Z. Anorg. Allg. Chem.* **1998**, *624*, 1285–1290. **DOI:**10.1002/(SICI)1521-3749(199808)624:8<1285::AID-ZAAC1285>3.0.CO;2-5
46. S.-J. Liu, C. Cao, C.-C. Xie, T.-F. Zheng, X.-L. Tong, J.-S. Liao, J.-L. Chen, H.-R. Wen, Z. Chang, X.-H. Bu, *Dalton Trans*. **2016**, *45*, 9209–9215. **DOI:**10.1039/C6DT01349J
47. R.-P. Li, Q.-Y. Liu, Y.-L. Wang, C.-M. Liu, S.-J. Liu, *Inorg. Chem. Front.* **2017**, *4*, 1149–1156. **DOI:**10.1039/C7QI00178A
48. T.-F. Zheng, S.-L. Yao, C. Cao, S.-J. Liu, H.-K. Hu, T. Zhang, H.-P. Huang, J.-S. Liao, J.-L. Chen, H.-R. Wen, *New J. Chem*. **2017**, *41*, 8598–8603. **DOI:**10.1039/C7NJ01463E

Povzetek

S hidrotermalno sintezo smo pripravili 4*f*–5*d* material ($HgDy_6Br_{12}$)Hg_8Br_{24} (**1**) in ga strukturno okarakterizirali z rentgensko monokristalno analizo. Spojine **1** ima dvodimenzionalno plastovito strukturo. Fotoluminiscenca v trdnem stanju kaže močno emisijo v modrem območju. Ozek optični pasovni razmik 1.97 eV je bil določen z UV/Vis difuzno refleksijo v trdnem. Magnetna susceptibilnost pri različnih temperaturah je v skladu z Curie-Weissovim zakonom ($c_m = c/(T-q)$) z C = 0.78 K in z Weissovo konstanto θ = –0.38 K, kar kaže na obstoj antiferomagnetnih interakcij.